

Moisture diffusivities evaluated at high moisture levels from a series of water absorption tests

M. Janz

Division of Building Materials, Lund University, Box 118, SE-22100 Lund, Sweden

(Now at Swedish Cement and Concrete Research Institute (CBI), SE-100 44 Stockholm, Sweden)

Paper received: August 31, 2000; Paper accepted: November 30, 2001

A B S T R A C T

This paper presents measured moisture diffusivities for sedimentary calcareous sandstone, lime silica bricks, bricks, and autoclaved, aerated concrete. The moisture diffusivities were calculated from the relation between the water sorption coefficients and the initial water content in the specimen before testing. The method used is based on Boltzmann transformation. The relation between the water sorption coefficients and the initial water content is measured by letting specimens, preconditioned to different initial water contents, suck de-ionized water while the water uptake is measured.

R É S U M É

Ce document présente les diffusivités d'humidité mesurées pour des grès calcaires sédimentaires, des briques silico-calcaïques, des briques et du béton cellulaire autoclavé. Les diffusivités d'humidité ont été calculées sur la base du rapport entre les coefficients de sorption d'eau et la teneur en eau initiale de l'échantillon avant les essais. La méthode utilisée repose sur la transformation de Boltzmann. Le rapport entre les coefficients de sorption d'eau et la teneur en eau initiale est mesuré en laissant les échantillons, préconditionnés selon différentes teneurs en eau initiales, s'imbiber d'eau déminéralisée pendant que l'absorption d'eau est mesurée.

1. INTRODUCTION

Durability problems such as frost attack, steel corrosion, timber rot, and mold are associated with high moisture content in materials. These durability problems cost society considerable sums each year. It is therefore important to be able to accurately predict the service life of materials, which necessitates calculating moisture movement in the materials. In order to calculate the moisture transport, the moisture diffusivity D_w [m^2/s] at high moisture levels must be known.

Moisture diffusivity can be calculated from transient moisture distributions. Various techniques can be used to measure these distributions, including nuclear magnetic resonance (NMR), gamma-ray attenuation, and thermal imaging. Measurements and laboratory arrangements for NMR are shown in [1-4]; for gamma-ray attenuation in [5-7] and for thermal imaging in [8-10]. All of these methods of measuring transient moisture profiles require major technical effort. There is a need for a method of determining transport coefficients more simply and easily.

Such a method is presented and used in this paper. Moisture diffusivities are calculated using the measured relation between the water sorption coefficients A [$\text{kg}/(\text{m}^2 \cdot \text{s}^{1/2})$], and the initial water content in the specimen before testing, w_{in} [kg/m^3]. Sorption coefficients are obtained by weighing the specimen in a number of capillary absorption tests. In principle, the only equipment needed to perform the capillary absorption test is a balance.

2. METHOD OF CALCULATING MOISTURE DIFFUSIVITY

The moisture diffusivity, D_w [m^2/s] is calculated using a measured relation between the sorption coefficient and the initial water content, $A(w_{in})$, and the water content at capillary saturation, w_{cap} [kg/m^3]. The sorption coefficient A [$\text{kg}/(\text{m}^2 \cdot \text{s}^{1/2})$] is defined by:

$$W = A\sqrt{t} \quad (1)$$

where W is the amount of absorbed water [kg/m^2] and t is the absorption time [s].

Editorial Note

The CBI is a RILEM Titular Member.

The method assumes that Fick's law describes the moisture flux, g [kg/(m²·s)]:

$$g = -D_w \frac{\partial w}{\partial x} \quad (2)$$

It is also assumed that moisture diffusivity is a step-wise constant within a certain range of water contents:

$$D_w(w) = \begin{cases} D_1 : w_{cap} > w > w_1 \\ D_2 : w_1 > w > w_2 \\ \vdots \\ D_N : w_{N-1} > w > w_N \end{cases} \quad (3)$$

The method used to evaluate moisture diffusivity is based on Boltzmann transformation. The moisture diffusivity is calculated using the relation between the sorption coefficient, A , and the initial water content, w_{in} . The Boltzmann transformation gives an analytical solution for a step response in semi-infinite volume. This method of evaluation was first presented in [11].

N values of initial water contents, $w_{in} = w_1, w_2, \dots, w_N$, with the N corresponding values of sorption coefficients, $A = A_1, A_2, \dots, A_N$, are selected from a measured relation $A(w_{in})$. Using these values, and knowing the water content at capillary saturation, w_{cap} , it is possible to determine the moisture diffusivity, $D_w = D_1, D_2, \dots, D_N$.

D_1 is calculated from the first interval w_1 to w_{cap} :

$$w_{cap} - w_1 = \frac{\sqrt{\pi} A_1}{2\sqrt{D_1}} \quad (4)$$

D_2 is calculated in the second interval w_2 to w_1 . Here $\eta_{2,1}$ is defined by step 1 and the moisture diffusivity, D_2 , is defined by step 2:

$$1. w_{cap} - w_1 = \frac{\sqrt{\pi} A_2}{2\sqrt{D_1}} \cdot \operatorname{erf}\left(\frac{\eta_{2,1}}{\sqrt{D_1}}\right) \quad (5a)$$

$$2. w_1 - w_2 = \frac{\sqrt{\pi} A_2}{2\sqrt{D_2}} \cdot e^{\left(-\eta_{2,1}^2 \left(\frac{1}{D_1} - \frac{1}{D_2}\right)\right)} \cdot \operatorname{erfc}\left(\frac{\eta_{2,1}}{\sqrt{D_2}}\right) \quad (5b)$$

$\eta_{2,1}$ shows the penetration depth, x , of the level $w = w_1$ at the time, t [11, 12]:

$$w = w_1 \text{ at } x = 2\eta_{2,1}\sqrt{t} \quad (6)$$

D_3 is calculated in three steps with A_3, w_3, D_1 and D_2 . This procedure is repeated until D_N is calculated in N steps. Step 1 to step $N-1$ gives $\eta_{N,1}$ to $\eta_{N,N-1}$ (each calculation gives new values $\eta_{N,i}$; these values do not show the penetration depth as $\eta_{2,1}$ does) and step N gives D_N :

$$1. w_{cap} - w_1 = \frac{\sqrt{\pi} A_N}{2\sqrt{D_1}} \cdot \operatorname{erf}\left(\frac{\eta_{N,1}}{\sqrt{D_1}}\right) \quad (7a)$$

$$2. w_1 - w_2 = \frac{\sqrt{\pi} A_N}{2\sqrt{D_2}} \cdot e^{\left(-\eta_{N,1}^2 \left(\frac{1}{D_1} - \frac{1}{D_2}\right)\right)} \cdot \left(\operatorname{erf}\left(\frac{\eta_{N,2}}{\sqrt{D_2}}\right) - \operatorname{erf}\left(\frac{\eta_{N,1}}{\sqrt{D_2}}\right)\right) \quad (7b)$$

$$\begin{aligned} & \vdots \\ N-1. & w_{N-2} - w_{N-1} = \frac{\sqrt{\pi} A_N}{2\sqrt{D_{N-1}}} \cdot e^{\left(-\eta_{N,1}^2 \left(\frac{1}{D_1} - \frac{1}{D_2}\right) - \dots - \eta_{N,N-2}^2 \left(\frac{1}{D_{N-2}} - \frac{1}{D_{N-1}}\right)\right)} \\ & \quad \cdot \left(\operatorname{erf}\left(\frac{\eta_{N,N-1}}{\sqrt{D_{N-1}}}\right) - \operatorname{erf}\left(\frac{\eta_{N,N-2}}{\sqrt{D_{N-1}}}\right)\right) \end{aligned} \quad (7N-1)$$

$$\begin{aligned} N. & w_{N-1} - w_N = \frac{\sqrt{\pi} A_N}{2\sqrt{D_N}} \cdot e^{\left(-\eta_{N,1}^2 \left(\frac{1}{D_1} - \frac{1}{D_2}\right) - \dots - \eta_{N,N-1}^2 \left(\frac{1}{D_{N-1}} - \frac{1}{D_N}\right)\right)} \\ & \quad \cdot \operatorname{erfc}\left(\frac{\eta_{N,N-1}}{\sqrt{D_N}}\right) \end{aligned} \quad (7N)$$

2.1 Numerical solution

A computer program developed by [13] can be used to solve Equations (4) to (7). The program uses the numerical solution presented by [11] and [13]. D_1 is calculated using Equation (4):

$$D_1 = \frac{\pi A_1^2}{4(w_{cap} - w_1)^2} \quad (8)$$

As shown in Equation (5), D_2 is calculated in two steps. In the first step, $\eta_{2,1}$ is calculated by the inverse function of $\operatorname{erf}(x)$. Equation (5a) gives:

$$\eta_{2,1} = \sqrt{D_1} \cdot \operatorname{erf}^{-1}\left(\frac{2\sqrt{D_1}(w_{cap} - w_1)}{\sqrt{\pi} A_2}\right) \quad (9)$$

In the second step D_2 is calculated from Equation (5b). This equation can be written so that all coefficients on the left-hand side of the equality are known and equal to K :

$$\begin{aligned} K &= \frac{2(w_1 - w_2)}{A_2} \cdot e^{\frac{\eta_{2,1}^2}{D_1}} \cdot \eta_{2,1} \\ &= \sqrt{\pi} \cdot \frac{\eta_{2,1}}{\sqrt{D_2}} \cdot e^{\frac{\eta_{2,1}^2}{D_2}} \cdot \operatorname{erfc}\left(\frac{\eta_{2,1}}{\sqrt{D_2}}\right) \end{aligned} \quad (10)$$

In order to solve this equation, a function $e_1(x)$ is introduced. By using this function in Equation (10), D_2 can be solved:

$$K = e_1\left(\frac{\eta_{2,1}}{\sqrt{D_2}}\right) \Rightarrow D_2 = \left(\frac{\eta_{2,1}}{e_1^{-1}(K)}\right)^2 \quad (11)$$

$e_1^{-1}(y)$ is the inverse of the introduced function $e_1(x)$. $e_1(x)$ is defined by (see Fig. 1):

$$e_1(x) = \sqrt{\pi} x e^{x^2} \cdot \operatorname{erfc}(x) \quad (12)$$

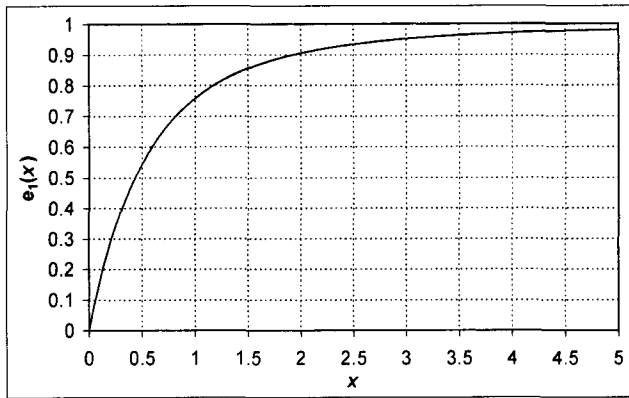


Fig. 1 – The function $e_1(x)$.

In the general case, with $n = 2, 3, \dots, N$, D_N is calculated using Equation (7). As in the case with two levels, Equation (7) is written so that all coefficients on the left-hand side of the equality are known and equal to K :

$$K = \frac{2(w_{N-1} - w_N)}{A_N} \cdot e^{\left(\eta_{N,1}^2 \left(\frac{1}{D_1} - \frac{1}{D_2}\right) + \dots + \eta_{N,N-1}^2 \frac{1}{D_{N-1}}\right)} \cdot \eta_{N,N-1} = e_1\left(\frac{\eta_{N,N-1}}{\sqrt{D_N}}\right) \quad (13)$$

Given the inverse function of $e_1(x)$, D_N is calculated:

$$D_N = \left(\frac{\eta_{N,N-1}}{e_1^{-1}(K)}\right)^2 \quad (14)$$

2.2 Reliability of the numerical method of evaluating moisture diffusivity

In order to check the reliability of the method described above, the water absorption and consequently also the sorption coefficients (A) for three different fictitious materials were calculated from a relation between the moisture diffusivity and the water content. Water absorption was calculated using a version of the well-documented computer program JAM-1 [14]. The relation between the moisture diffusivity and the water content of the fictitious materials, and the calculated sorption coefficients, are shown in Table 1.

Thereafter, “new” moisture diffusivities were calculated from the calculated sorption coefficients using the numerical solution described above. These results are shown in Table 2. The difference between the moisture diffusivity used for input and the output is, as would be expected, very small (less than 1% for Material 1 and Material 2). This error is probably negligible in comparison with the errors in experimental measurement of sorption coefficients. Material 3 has very non-linear moisture diffusivity, which probably accounts for the slightly larger deviation of the moisture diffusivities calculated for it.

3. MATERIALS

The materials tested were Gotland sandstone, autoclaved aerated concrete, lime silica brick and brick. Gotland sandstone is a sedimentary calcareous sandstone

that was often used as a building material in the Baltic region during the seventeenth and eighteenth centuries.

To be able to calculate the moisture content mass per volume from the moisture content mass by mass, the dry bulk density has to be known. The density was determined using Archimedes’ principle: the specimen was vacuum-saturated with water and weighed in air and in water. The volume and

bulk density were calculated from:

$$V = \frac{m_{air} - m_w}{\rho_w} \quad (15)$$

$$\rho = \frac{m_0}{V} \quad (16)$$

where V is the specimen volume [m^3], m_{air} is the vacuum saturated specimen weight in air [kg], ρ_w is the density of water [kg/m^3] ρ is the

w [kg/m^3]	Material 1		Material 2		Material 3	
	D_w [m^2/s]	A [$kg/(m^2 \cdot s^{1/2})$]	D_w [m^2/s]	A [$kg/(m^2 \cdot s^{1/2})$]	D_w [m^2/s]	A [$kg/(m^2 \cdot s^{1/2})$]
0		9.865		19.547		31.759
1	1	8.042	2	16.085	1	26.943
2	2	5.862	8	11.724	2	21.072
3	4	3.191	16	6.382	8	12.764
4	8	0	32	0	128	0

w [kg/m^3]	D_w [m^2/s], Material 1	D_w [m^2/s], Material 2	D_w [m^2/s], Material 3
0-1	1.004 (0.4%)	2.010 (0.5%)	1.089 (8.9%)
1-2	2.000 (0%)	8.013 (0.16%)	2.123 (6.2%)
2-3	3.998 (0.05%)	15.992 (0.05%)	8.054 (0.68%)
3-4	7.997 (0.04%)	31.989 (0.03%)	127.957 (0.03%)

density of the specimen [kg/m³] m_w is the vacuum saturated specimen weight in water [kg] m_0 is the dry weight [kg].

The weighing in air and water also enables determination of the porosity, P [m³/m³], and the solid density, ρ_s :

$$P = \frac{m_{air} - m_0}{\rho_w \cdot V} \quad (17)$$

$$\rho_s = \frac{\rho}{1 - P} \quad (18)$$

The capillary porosity, P_{cap} , and the moisture content at capillary saturation, w_{cap} , were also evaluated from capillary water uptake tests performed on specimens dried at 105°C and exposed to one-side water absorption. Capillary water saturation is defined as the moisture content when the capillary water uptake comes to an almost complete halt. Capillary porosity is defined as the water-filled porosity at that time (see Fig. 2). However, the moisture content continues to increase even after rapid capillary suction has stopped. This increase is due to air in pores that are non-active during capillary suction dissolving in the water. This process is, however, very slow, and is not considered in this paper.

The bulk density, solid density, porosity, capillary porosity, and the moisture content at capillary saturation of the tested materials are shown in Table 3.

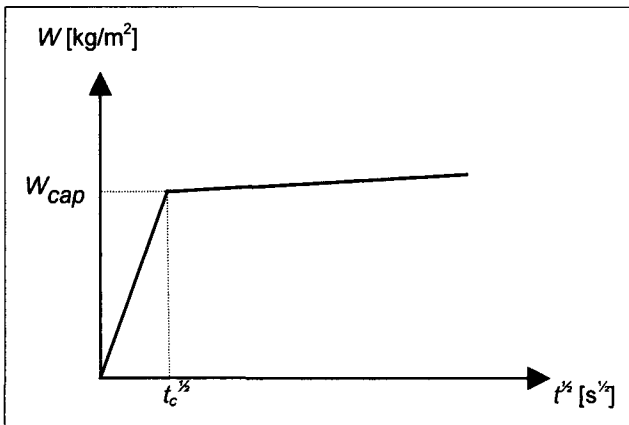


Fig. 2 – Capillary water uptake test used for determination of capillary water saturation and capillary porosity. The initial rapid water uptake comes to an end when capillary transport stops. The moisture content continues to increase as a consequence of the air in non-active pores dissolving in the water. This latter process is, however, very slow.

4. EXPERIMENTAL METHOD

4.1 General

The purpose of the experimental work is to find a relation between the water sorption coefficient, A [kg/(m²·s^{1/2})] and the initial moisture content in the specimens before testing, w_{in} [kg/m³]. This relation $A(w_{in})$ is then used to calculate the moisture diffusivity D_w [m²/s]. In order to obtain the relation $A(w_{in})$, the specimens were conditioned to different desired initial water contents in both the hygroscopic (up to approximately 98% relative humidity) and the superhygroscopic ranges. The water sorption coefficients were then measured by letting the preconditioned specimens suck water. For all specimens except the autoclaved aerated concrete, the amount of water absorbed was recorded automatically by a computer.

4.2 Preconditioning

The conditioning procedure started with drying the specimens until no changes in weight were observed, whereupon the dry weight was determined. Thereafter the specimens absorbed water to the desired water content. Once the desired moisture content had been reached, the specimens were wrapped in plastic film and stored for at least 14 days in a climate chamber to achieve as homogenous moisture content as possible. A water-filled container was placed in the climate chamber with the specimens in order to keep the relative humidity in the chamber as close to 100% as possible, so preventing moisture loss from the specimens through the plastic during the storage time.

For the Gotland sandstone, two methods of preconditioning the specimens were compared to the method described above, namely well-defined conditioning through absorption and desorption in the hygroscopic range and through desorption in the superhygroscopic range. In the hygroscopic range saturated salt solutions were used to obtain different relative humidity. Above the hygroscopic range, pressure plate and pressure membrane extractors were used to condition the specimen. These two methods will probably not give rise to any moisture gradient in the specimen.

4.3 Absorption test

All specimens except the autoclaved aerated concrete absorbed de-ionized water from a reservoir during the capillary water uptake test. The specimens were connected to the reservoir through the nozzle and a liquid supply system (see Fig. 3). A balance recorded the loss of weight of the water reservoir and the readings were transmitted to a computer, which could record data at one-second intervals. In order to prevent evaporation from the water reservoir,

Material	ρ [kg/m ³]	ρ_s [kg/m ³]	P [%]	P_{cap} [%]	w_{cap} [kg/m ³]
Gotland sandstone	2059	2674	23	16	160
Autoclaved aerated concrete	490	2608	81	36	365
Lime silica brick	1874	2641	29	24	237
Brick	1976	2670	26	19	187

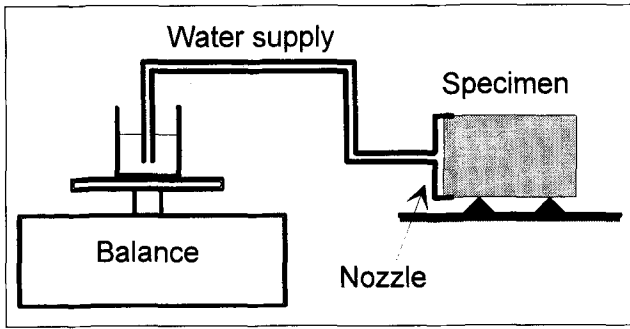


Fig. 3 – Schematic presentation of the laboratory set-up. To prevent evaporation from the water reservoir, the balance was placed in a small chamber with approximately 100% relative humidity.

the balance was placed in a small chamber with approximately 100% relative humidity. At the start of the capillary water uptake test, air was evacuated from the water supply system and the nozzle through a valve on the nozzle. This resulted in wetting of the entire end of the specimen. The nozzle was designed in such a way that the whole specimen surface was wetted within a few seconds. During the test the specimen was positioned horizontally.

The autoclaved aerated concrete was tested by placing the specimen in a container with de-ionized water and allowing it to suck water from one side. Thus in this case the direction of absorption was vertical. The amount of absorbed water was registered by weighing the specimen at regular intervals.

5. RESULTS AND DISCUSSION

As described the sorption coefficient was measured by letting a preconditioned specimen suck water while electronically monitoring the amount of water absorbed. The amount of absorbed water per square meter was plotted as a function of the square root of time. Fig. 4 shows a typical result from such measurements (here using a sample of the Gotland sandstone).

The decreasing slope at the end of the curve is caused by gradual capillary saturation of the specimen. The slope of the linear part of the function gives the sorption coefficient, $A(w_{in})$ (see Fig. 5).

Fig. 6 shows sorption coefficients for Gotland sandstone as a function of the initial water content. Apart from the results presented here, the effect of initial water content on the water sorptivity is studied in [15, 16]. Each point in Fig. 6 corresponds to one capillary water uptake test. Besides the normal preconditioning procedure, the specimens were conditioned in the hygroscopic range in climate boxes, and in the superhygroscopic range by a pressure plate extractor (for pressures up to 15 bar) and a pressure membrane extractor (for pressures up to 100 bar). No significant differences were found between specimens conditioned using different methods. This finding indicates that there is no moisture gradient over the specimen volume after the normal

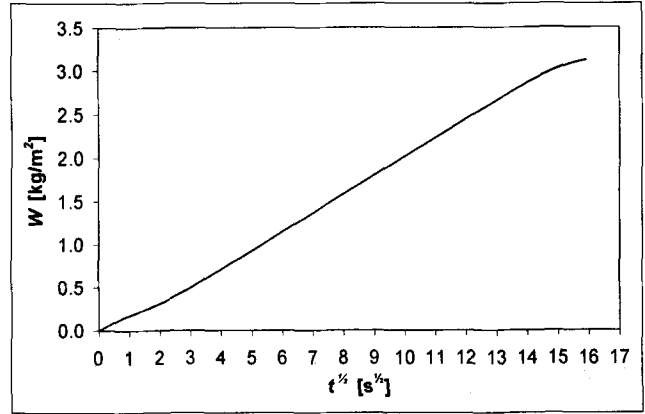


Fig. 4 – The amount of absorbed water per square meter W , is drawn as a function of the square root of time (here as measured on Gotland sandstone).

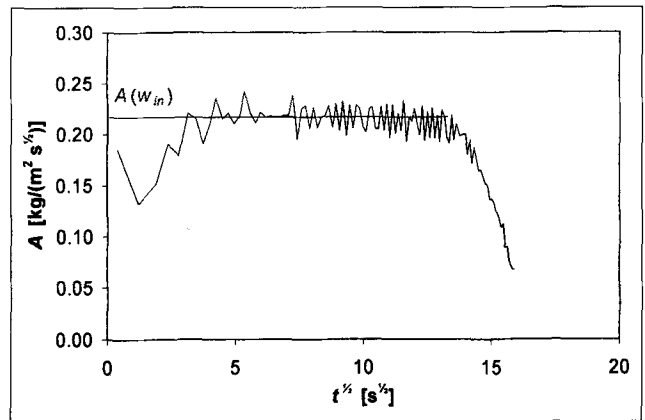


Fig. 5 – The slope of the curve in Fig. 4; the sorption coefficient A , is approximately $0.22 \text{ kg}/(\text{m}^2 \cdot \text{s}^{1/2})$.

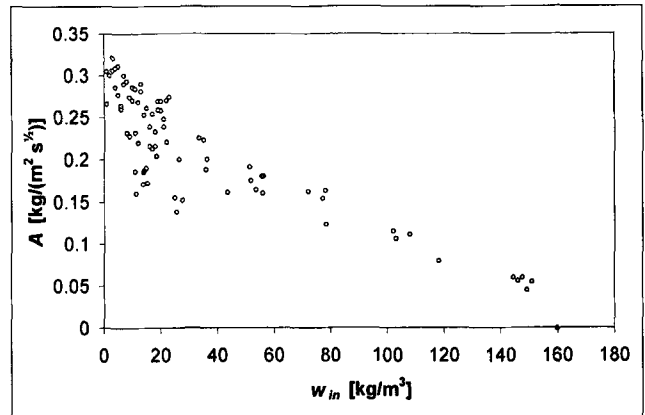


Fig. 6 – The sorption coefficient A , as a function of the initial water content expressed as mass by volume, w_{in} , for Gotland sandstone. Each point represents one capillary water uptake test. The capillary saturation, w_{cap} , is approximately $160 \text{ kg}/\text{m}^3$.

conditioning procedure. Therefore, the normal conditioning procedure seems to be sufficient.

The moisture diffusivity was calculated from the relation between the moisture content and the sorption coefficient $A(w_{in})$ using the theory and numerical model described above. The input data were chosen from the measured relations $A(w_{in})$ and is shown in Table 4. Fig. 6

Table 4 – The input data, i.e. the initial moisture contents w_{in} and the sorption coefficients A , used for the calculations of the moisture diffusivity

Gotland sandstone		Aerated autoclaved concrete		Lime silica brick		Brick	
w_{in} kg/m ³	A kg/(m ² ·s ^{1/2})	w_{in} kg/m ³	A kg/(m ² ·s ^{1/2})	w_{in} kg/m ³	A kg/(m ² ·s ^{1/2})	w_{in} kg/m ³	A kg/(m ² ·s ^{1/2})
160	0	365	0	237	0	187	0
159	0.01201	356	0.01641	220	0.00792	185.8	0.01984
158	0.01947	344	0.03078	200	0.01533	183	0.04498
156	0.02916	320	0.04916	180	0.02110	178	0.07142
154	0.03646	285	0.06802	160	0.02586	173	0.09108
150	0.04794	208	0.09881	60	0.04366	165	0.11579
140	0.06919	130	0.12391	30	0.06053	155	0.14087
80	0.14594	0	0.15909	0	0.08123	145	0.16203
40	0.18179					127	0.19444
20	0.19712					100	0.23502
0	0.25932					59.5	0.28553
						0	0.34741

shows an example of the measured relation between the sorption coefficient and initial moisture content.

Figs. 7 to 10 show the calculated moisture diffusivities. For both the Gotland sandstone and the lime silica

brick, disproportionately high moisture diffusivities are produced at low moisture levels. It is possible that this is an inaccuracy, and that a different driving potential, such as suction, might have shown the relations increasing steadily. However, the moisture diffusivities of the Gotland sandstone and of the lime silica brick at low moisture levels do not influence the calculated values at high moisture levels, even if they are incorrect. This is due to the fact that the calculation starts at capillary saturation. Consequently moisture diffusivities at high moisture levels are always the most reliable.

When calculating the moisture diffusivity, $\text{erf}(x)$ is inverted in Equation (9) and the function $e_1(x)$ is inverted in Equations (11) and (14). These two inversions limit the possible choices of input values since $-1 < \text{erf}(x) < 1$ and

$e_1(x) < 1$. Therefore, the conditions that must be fulfilled in Equation (9) are:

$$-1 < \left(\frac{2\sqrt{D_1} \cdot (w_{cap} - w_1)}{\sqrt{\pi} A_2} \right) < 1 \tag{19}$$

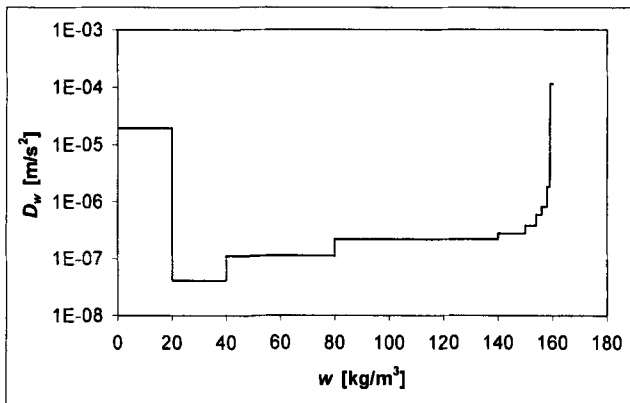


Fig. 7 – Moisture diffusivity obtained on the Gotland sandstone.

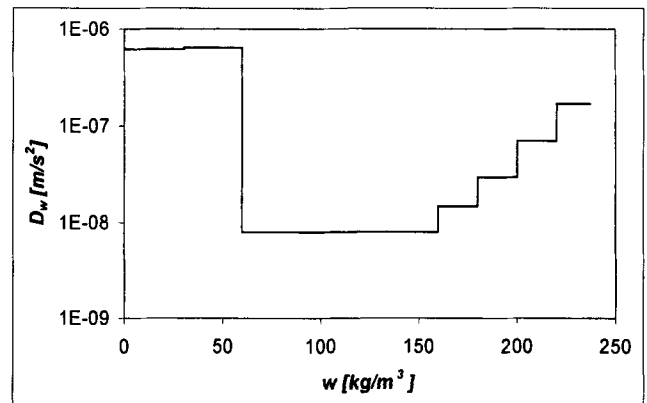


Fig. 9 – Moisture diffusivity obtained on the lime silica brick.

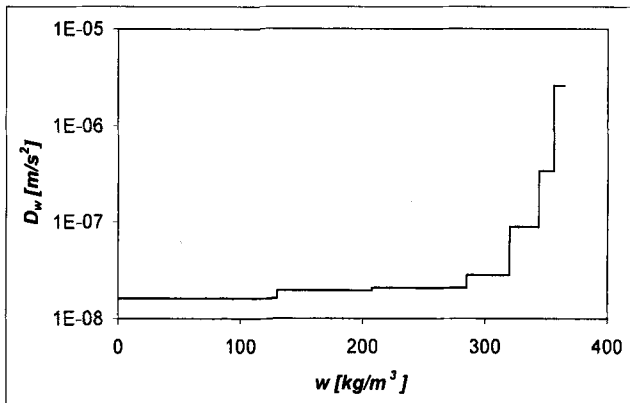


Fig. 8 – Moisture diffusivity obtained on the aerated autoclaved concrete.

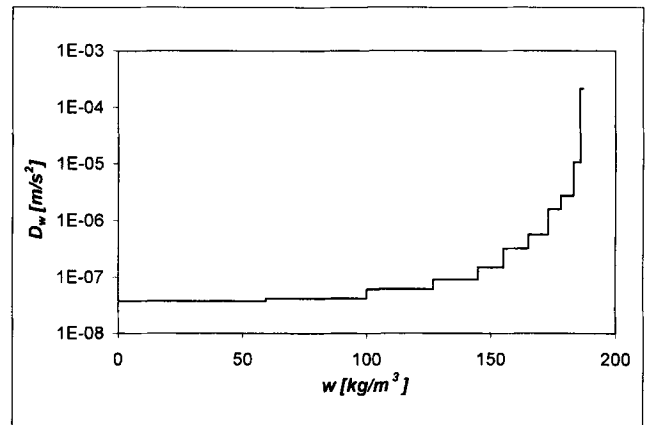


Fig. 10 – Moisture diffusivity obtained on the brick.

and for Equations (11) and (14):

$$K = \frac{2(w_{N-1} - w_N)}{A_N} \cdot e^{\left(\eta_{N,1}^2 \left(\frac{1}{D_1} - \frac{1}{D_2}\right) + \dots + \eta_{N,N-1}^2 \frac{1}{D_{N-1}}\right)} \cdot \eta_{N,N-1} < 1 \quad (20)$$

As shown above, the calculation of the moisture diffusivity $D(w)$ starts at capillary saturation. Then gradually lower initial water contents are used. This means that the first input value chosen, (w_1, A_1) , determines the possible choices among the rest of the input values. The limitations on possible input entailed by Equations (19) and (20) can, in some cases, make the evaluation quite arduous. Very small changes in the chosen input values can result in that limitations being met or unmet.

5.1 Reliability of the method

The best way to check the reliability of the method used is to compare measured moisture distributions during a water absorption experiment with calculated distributions. Of the materials tested, moisture distributions were only measured on the brick [17]. The measurements were performed using thermal imaging. Fig. 11 shows both the calculated and measured distributions. The distributions were calculated using a combination of Fick's law (Equation (2)) and conservation of mass:

$$\frac{\partial w}{\partial t} = \frac{\partial}{\partial x} \left(D_w \frac{\partial w}{\partial x} \right) \quad (21)$$

The calculations are performed with the computer program JAM-1 [14] using the moisture diffusivities shown in Fig. 10. It should be pointed out that the measured distributions were measured on only three individual specimens after 0.5, 1 and 2 hour's capillary absorption using dry specimens. Thus the spread between the measured results is probably high. However, the agreement between measured and calculated moisture distributions is good, especially after 0.5 and 1 hours.

As said, moisture distributions were only measured on the brick. However, moisture diffusivities of lime silica brick, obtained by three different laboratories from measurement of transient moisture distributions using gamma-ray attenuation and NMR are reported in [18]. The material used was not identical to the lime silica brick tested here, but both the density and the porosity were similar. Therefore, the magnitude of the calculated moisture diffusivities should also be similar. As is clear from Fig. 12, this is in fact the case from $w_{in}/w_{cap} \approx 0.2$ up to capillary saturation. This establishes that the reliability of the proposed method of evaluating moisture diffusivities appears to be high.

6. CONCLUSIONS

Existing methods of measuring moisture diffusivities from measured transient moisture distributions with NMR or gamma ray attenuation are cost-intensive. There

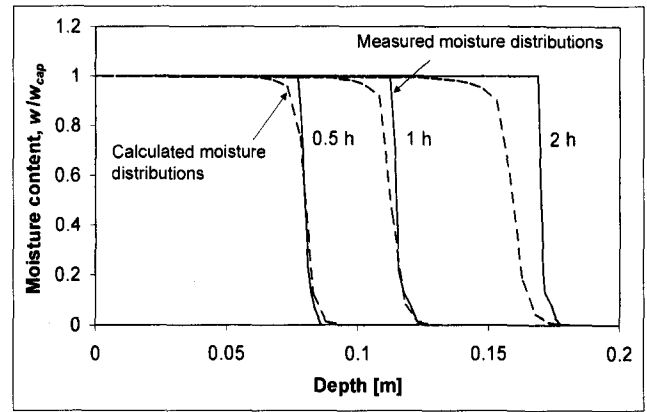


Fig. 11 – Measured and calculated moisture distributions [17].

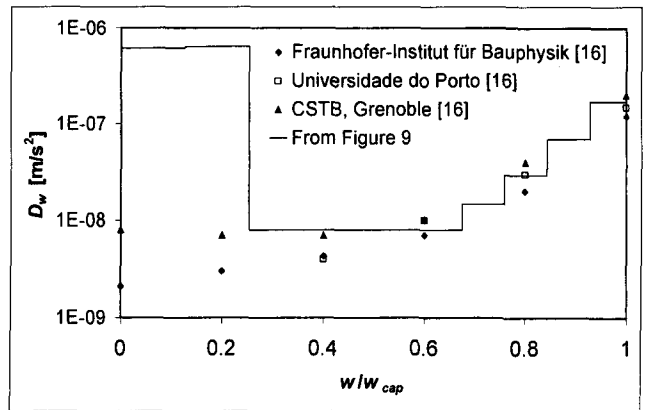


Fig. 12 – Moisture diffusivity obtained on the lime silica brick. Moisture diffusivities of a similar lime silica brick evaluated from transient moisture distributions measured by three different laboratories with gamma-ray attenuation and NMR in [18].

is an obvious need for a simple complementary method. The method presented here is such a method. The only more costly equipment needed is a balance used for the measurements and a computer for the evaluation process.

This new technique for measuring and evaluating the relation between moisture diffusivity and moisture content, $D(w)$ is accurate provided that the moisture diffusivity is a stepwise constant within a certain range of water contents and that Fick's law describes the moisture flux. It has been shown that the error introduced with the numerical solution used is minor. The largest source of error is the experimental determination of sorption coefficients. These experiments are, however, relatively easy to perform.

However, because evaluation starts at capillary saturation and the result of the previous calculation is used as input in the next calculation at a slightly lower moisture level, possible errors introduced in previous calculations will be transmitted. Thus, the higher the moisture level, the more reliable the moisture diffusivities evaluated on the Gotland sandstone, autoclaved aerated concrete, lime silica brick, and brick. At low moisture contents there are well-established test methods, such as the cup method, that can complement the moisture diffusivities evaluated at high moisture levels. Hence, the method presented here and the cup method might form a power-

ful combination for determining moisture diffusivities in the whole moisture range up to capillary saturation.

Moisture distributions calculated with measured moisture diffusivities and distributions measured with thermal imaging on the brick show good agreement. Furthermore it has been shown that moisture diffusivities obtained for the lime silica brick at high moisture levels are of the same magnitude as moisture diffusivities evaluated from measured transient moisture distributions for a similar lime silica brick. Thus, the reliability of the method seems to be high.

ACKNOWLEDGEMENTS

The support of the Swedish Council for Building Research and the Development Fund of the Swedish Construction Industry is gratefully acknowledged. The author also wishes to express his gratitude to Professor Johan Claesson, who first developed the idea of evaluating moisture diffusivities in the way presented in this paper.

REFERENCES

- [1] Kopinga, K. and Pel, L., 'One-dimensional scanning of moisture in porous materials with NMR', *Rev. Sci. Instrum.* **65** (1994) 3673-3681.
- [2] Pel, L., 'Moisture transport in porous building materials', Eindhoven University of Technology, 1995.
- [3] Krus, M., 'Moisture transport and storage coefficients of porous mineral building materials: Theoretical principles and new test methods' (in German), PhD Dissertation, University of Stuttgart, 1995.
- [4] Brocken, H. J. P., 'Moisture transport in brick masonry: the gray area between bricks', Brocken PhD thesis, Eindhoven University of Technology, 1998.
- [5] Wormald, R. and Britch, A. L., 'Methods of measuring moisture content applicable to building materials', *Building Science* **3** (1969) 135-145.
- [6] Nielsen, A. F., 'Gamma-ray-attenuation used for measuring the moisture content and homogeneity of porous concrete', *Building Science* **7** (1972) 257-263.
- [7] Quénard, D. and Sallee, H., 'A gamma-ray spectrometer for measurement of the water diffusivity of cementitious materials', Proceedings of Materials Research Symposium, Boston, 28-30 November 1989, Vol. 137, 165-169.
- [8] Sosoro, M. and Reinhardt, H. W., 'Thermal imaging of hazardous organic fluids in concrete', *Mater. Struct.* **28** (183) (1995) 526-533.
- [9] Sosoro, M., 'A model to predict the absorption of organic fluids in concrete' (in German), *Deutscher Ausschuss für Stahlbeton* **446** (1995) Beuth Verlag GmbH, Berlin.
- [10] Johansson, P., 'A thermal imaging method for measuring moisture distribution in porous building materials', Proceedings of the 5th Symposium on Building Physics in the Nordic Countries, Göteborg, August 24-26 1999, 297-304.
- [11] Claesson, J., 'Determination of moisture transport coefficients at very high moisture levels by a series of capillary absorption tests' (in Swedish), Division of Building Physics, Lund Institute of Technology, 1994.
- [12] Crank, J., 'The Mathematics of Diffusion', 2nd Edn. (Oxford University Press, 1975).
- [13] Arfvidsson, J. and Janz, M., 'Determination of moisture transport coefficients at very high moisture levels by a series of capillary absorption tests' (in Swedish), Part of Report TVBH-7180, Division of Building Physics, Lund Institute of Technology, 1994.
- [14] Arfvidsson, J., 'Computer model for moisture transport in porous materials. Manual for JAM-1.0' (in Swedish), Division of Building Physics, Lund Institute of Technology, 1988.
- [15] Schwarz, B., 'Capillary water absorption in building materials' (in German), *Gesundheits-Ingenieur* **7** (93) (1972) 206-211.
- [16] Hall, C., Hoff, W. D. and Skeldon, M., 'The sorptivity of brick: dependence on the initial water content', *Journal of Physics* **16** (1983) 1875-1880.
- [17] Janz, M. and Johansson, P., 'Moisture profiles measured with thermal imaging over an interface between cement-lime mortar and brick', Manuscript, Division of Building Materials, Lund Institute of Technology, 2000.
- [18] De Freitas, V. P., Krus, M., Künzle, H. and Quénard, D., 'Determination of the water diffusivity of porous materials by gamma-ray attenuation and NMR', Proceedings of the International Symposium on Moisture Problems in Building Walls, Porto, 11-13 Sept 1995, 445-460.